Quantum Chemical Study of Mechanisms for Oxidative Dehydrogenation of Propane on Vanadium Oxide

P. C. Redfern,[†] P. Zapol,[†] M. Sternberg,[†] S. P. Adiga,[†] S. A. Zygmunt,[†,‡] and L. A. Curtiss*[,†]

Materials Science and Chemistry Divisions, Argonne National Laboratory, Argonne, Illinois 60439, and Department of Physics and Astronomy, Valparaiso University, Valparaiso, Indiana 46383

Received: October 28, 2005; In Final Form: December 22, 2005

We have carried out a hybrid density functional study of mechanisms for oxidative dehydrogenation of propane on the (010) surface of V_2O_5. The surface was modeled using both vanadium oxide clusters and a periodic slab. We have investigated a Mars-van Krevelen mechanism that involves stepwise adsorption of the propane at an oxygen site followed by desorption of a water molecule and propene, and subsequent adsorption of an oxygen molecule to complete the catalytic cycle. The potential energy surface is found to have large barriers, which are lowered somewhat when the possibility of a triplet state is considered. The barriers for propane adsorption and propene elimination are 45−60 kcal/mol. The highest energy on the potential energy surface at the B3LYP/6-31G(*) level of theory is about 80 kcal/mol above the energy of the reactants and corresponds to formation of an oxygen vacancy after water elimination. Subsequent addition of an oxygen molecule to fill the vacancy is predicted to be energetically downhill. The reactions of propane at a bridging oxygen site and at a vanadyl site have similar energetics. The key results of the cluster calculations are confirmed by periodic calculations. Factors that may lower the barriers on the potential energy surface, including the interaction of vanadium oxide clusters with a support material and a concerted reaction with O_2, are discussed.

1. Introduction

The oxidative dehydrogenation (ODH) of propane over a supported vanadia catalyst is of great interest because of its importance in industrial catalysis.[1] The support is usually an oxide such as Al_2O_3, SiO_2, or TiO_2. Experimental studies of catalyst structure[2−5] generally agree that when the concentration of vanadium oxide species is low, isolated VO_4 units form on the support surface. These units are assumed to contain a vertical V═O double bond and three bridging V−O−S linkages, where S represents the support metal cation (S = Al, Si, Ti, etc.). If the catalyst is prepared with a higher concentration of vanadium oxide, larger V_2O_7 units are formed. These species appear to have two vertical V═O bonds, four bridging V−O−S linkages, and a new bridging V−O−V linkage. For increasing vanadium oxide concentrations, larger but similar units can be formed, up to the limit where the entire support surface is covered by a monolayer. The dependence of the reactivity on coverage of the support surface by vanadium oxide is unclear in the literature.[4,6]

Experimental studies of the ODH reaction with supported vanadia catalysts have generally supported the reaction mechanism originally proposed by Mars and van Krevelen.[7] This envisions the reaction happening in three basic steps. (1) An oxygen atom from the catalyst is inserted into a C−H bond of the propane molecule, which then binds to the catalyst surface. (2) The surface-bound propane forms propene and releases a water molecule. (3) An oxygen molecule present in the feed stream returns an oxygen atom to the catalyst to fill the vacancy left in the first step. Although this mechanism is consistent with most experimental studies, important questions remain to be answered. First, which oxygen atom is removed from the catalyst surface? Does it come from the vertical V═O vanadyl bond, as suggested by Oyama,[8] or from one of the bridging linkages (V−O−S or V−O−V), as described by Eon et al.[9] and Chen et al.?[10] Second, what is the rate-limiting step for the ODH reaction? Third, how does propane interact with the catalyst oxygen atom to form propene and water? Fourth, how does the support enhance the catalytic activity of vanadium oxide? There is strong evidence that step (3) is not rate-limiting, and the observed dependence of catalyst reactivity on the support material suggests that the V−O−S linkage may be involved in oxidation reactions,[11] but the details are not well understood because of the complexity of the catalyst surfaces.

There have been a number of computational studies of the electronic structure and bonding properties of clean vanadium oxide surfaces and supported vanadium oxide clusters,[12−20] and several computational studies have been reported on propane ODH on metal oxide surfaces with one of these on vanadium oxide. These propane ODH studies have been done on small cluster models of the metal oxide surfaces without inclusion of the metal oxide support. Gilardoni et al.[21] have investigated the reaction of propane on a cluster model of vanadium oxide without a support and the subsequent desorption of a water molecule using density functional theory. They investigated the adsorption of propane only at the vanadyl oxygen site and not at a bridging oxygen site. They used cluster models of two and four vanadium atoms and found the highest barrier on the reaction pathway to be about 15 kcal/mol. Experimental studies have shown that the activation barrier for propane ODH on supported vanadium oxide is 20−30 kcal/mol.[4,10,22] Fu et al.[23] have reported a density functional investigation of the initial activation of propane on molybdenum oxide. They used a cluster with three Mo atoms (Mo_3O_9) and investigated six possible mechanisms for C−H bond activation on the terminal M═O sites. They found that the methylene CH_2 group of propane is more reactive than the methyl CH_3 group and calculated activation enthalpies, which were in reasonable agreement with experiment. In a study of the interaction of methane with V_2O_5, Haber and Witko[24] found that cleavage of the C−H bond

[†] Argonne National Laboratory.
[‡] Valparaiso University.

10.1021/jp056228w CCC: $33.50
Published on Web 04/01/2006

proceeds via transfer of two electrons to empty vanadium surface levels and formation of adsorbed alkoxy and surface hydroxyl species.

The related partial oxidation reaction of methanol to formaldehyde has also been studied recently using computational methods. Khaliullin et al.[25] carried out a comparative study of the reaction energetics for a VO_4 active site supported on cluster models of the SiO_2, TiO_2, and ZrO_2 surfaces. They found activation energies that were significantly higher than those found experimentally, and also found little dependence of activation energy on the support material, which is also contrary to experiment. The authors concluded that isolated VO_4 units are not able to catalyze the reaction, but that pairs of adjacent VO_4 groups or dimeric V_2O_7 clusters may be required. Boulet et al.[26] used cluster models of the (010) V_2O_5 surface to map out the potential energy surface for the same reaction. They found that to obtain an activation energy in reasonable agreement with experiment, they had to assume that the desorption of formaldehyde occurred in a concerted mechanism involving an oxygen atom provided by the dissociative adsorption of molecular oxygen on the V_2O_5 surface. Without the assistance of such an oxygen species the reaction barrier was far higher than typical experimental values. However, the authors compared computational results for a V_2O_5 surface with experimental results for supported vanadium oxide, so it is not clear whether agreement is to be expected or not.

In the work reported here, we have carried out the first detailed theoretical study of the complete reaction pathway for propane ODH on a vanadium oxide surface following the steps of a Mars-van Krevelen mechanism. We considered two possible sites for C−H activation of propane based on reactions at both the vanadyl and bridging oxygen sites followed by hydrogen rearrangement on the surface that leads to the formation of propene and the desorption of water. The addition of oxygen to restore the metal oxide surface was also investigated. The calculations use the hybrid B3LYP density functional method and clusters with up to 10 vanadium atoms. In addition, periodic calculations of some of the points on the reaction surface were used to test the validity of the cluster model results. Our calculations suggest that the (010) surface of V_2O_5 is unfavorable for propane ODH and that other factors, such as the influence of a support material, are responsible for the experimentally observed catalytic activity of vanadia. The results of this study provide insight into questions concerning the activity of supported vanadia catalysts and provide the basis for future computational investigations of these materials. In section 2, the theoretical methods and models are described. Results and discussion of the reaction pathways for ODH of vanadium oxide are presented in section 3.

2. Computational Methods

Most of the cluster calculations reported in this paper were done using the hybrid B3LYP density functional method.[27] This functional has been found to be among the most accurate of the density-functional-based methods for the calculation of thermochemical data.[28,29] The 6-31G* basis set[30] without f-polarization functions on vanadium was used for geometry optimizations of stable equilibrium structures and transition states. This modified basis set is referred to as 6-31G(*) to denote that f-functions are not included on vanadium. Since vanadium is partially ionic in all of these calculations, there is little loss of variational freedom from the exclusion of the f-functions. Single point B3LYP calculations at the B3LYP/6-31G(*) geometries were also done with a larger basis set, G3MP2Large,[31,32] in order

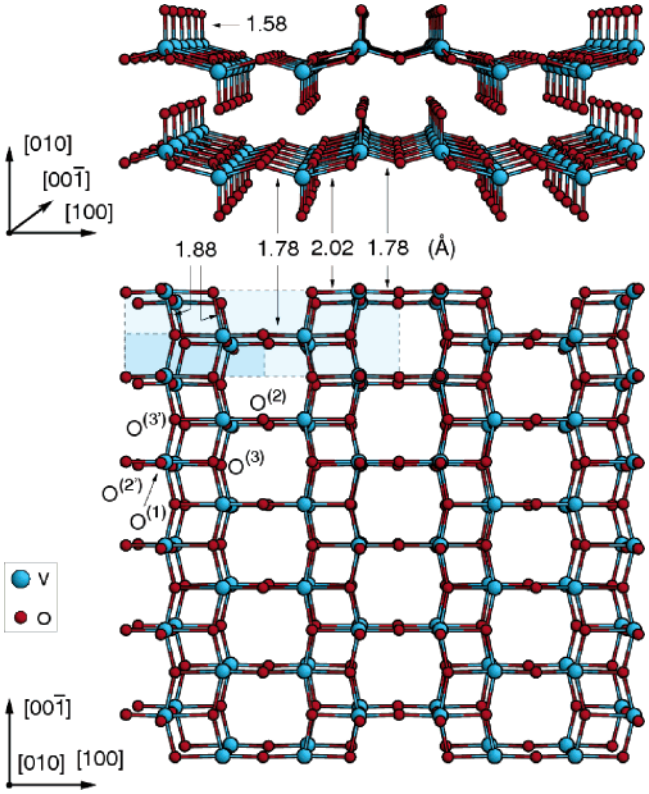

Figure 1. Structure of the (010) surface of V_2O_5.

to assess the 6-31G(*) results. The G3MP2Large basis set includes f and g functions on vanadium. It is equivalent to 6-311+G(2df,p) on C, O, H and 6-311+G(3f2g) on V. The Gaussian98 and Gaussian03 computer codes were used for all calculations.[33] The periodic calculations using the CRYSTAL03 code[34] were done using the B3PW91 density functional method with the 6-31G(*) basis set. This functional is similar in performance to B3LYP and was also used on some of the cluster calculations for comparison.

a. Cluster Models. Most of the calculations reported here were done using cluster models of the V_2O_5 (010) surface. The (010) surface was chosen because of the presence of the VO_4 and V_2O_7 structural units that are believed to be involved in supported vanadia catalysis. The (010) V_2O_5 surface, which is shown in Figure 1, was represented by five cluster models: VO_5H_5 (**V1**), $V_2O_9H_8$ (**V2**), $V_4O_{14}H_8$ (**V4**), $V_6O_{23}H_{16}$ (**V6**), and $V_{10}O_{31}H_{12}$ (**V10-A, V10−B**). The structures of these five clusters are shown in Figure 2. The experimental structure[35] with the $Pmn2_1$ space group was used to derive geometrical parameters for the clusters. In Figure 2 it is seen that one oxygen adjacent to each vanadium in the VO_5H_5 and $V_2O_9H_8$ models is capped with two hydrogens, reflecting the fact that in the crystal structure one of the five oxygens in the first coordination sphere of vanadium has bonds to two other vanadium atoms. This oxygen is further away than the others from vanadium [0.1−0.2 Å further than the V−O bonds and ∼0.5 Å further than the V═O (vanadyl) bond]. Also, a natural bond orbital (NBO)[36] analysis showed no localized covalent bond between this V, O pair. The terminating OH and OH_2 groups were frozen and standard 0.96 Å OH bond lengths were used. All of the interior V and O atoms in the $V_2O_9H_8$ and larger clusters were allowed to relax. In the VO_5H_5 cluster, only the V═O atoms were allowed to relax their positions.

Partial optimizations of all equilibrium structures on the potential energy surface were done within the geometry

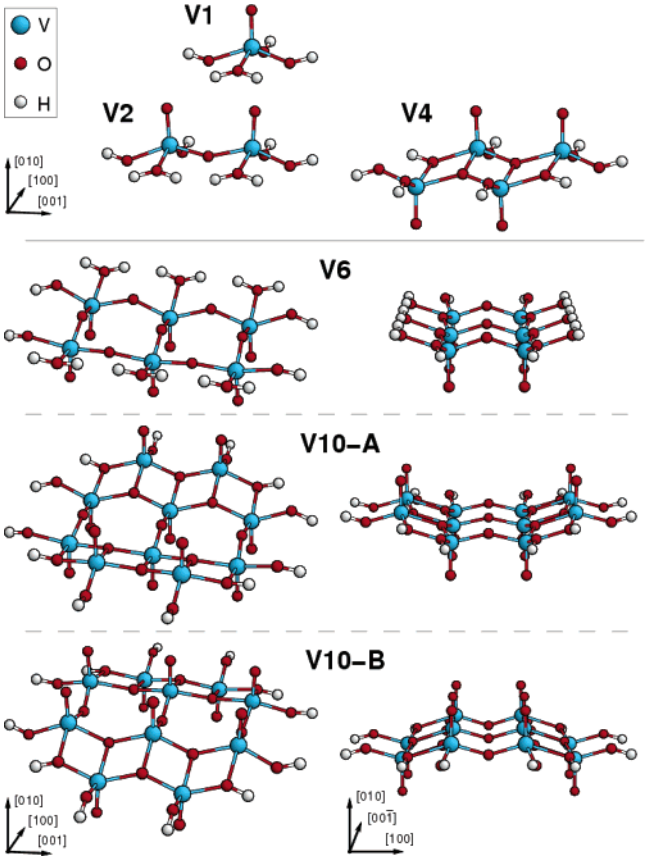

Figure 2. Structures of cluster models used to represent the (010) surface of V_2O_5: **V1** = $V_1O_5H_4$, **V2** = $V_2O_9H_8$, **V4** = $V_4O_{14}H_8$, **V6** = $V_6O_{23}H_{16}$, **V10-A, V10-B** = $V_{10}O_{31}H_{12}$. (**V10-B** is the same as **V10-A**, but is inverted. **V10-A** is used for modeling the reaction at the O(2) site, while V10-B is used to model the O(1) site.)

TABLE 1: Bond Lengths and Neighbor Distances (in Å) for V_2O_5 Cluster Models[a]

distance	V1	V2	V4	V6	V10	expt.[d]
V···V [001]		3.63	3.63	3.60	3.65	3.56
V···V [100]				3.39	3.46	3.43
V═O(1)	1.57	1.57	1.56	1.56	1.52	1.59
V−O(2)	1.75	1.76	1.77	1.78	1.78	1.78
V−O(3)	1.91	1.89	1.88[b]	1.89	1.90[b]	1.88
			1.97[c]		1.94[c]	
V···O(3)	2.10	2.14	2.04	2.12	2.00	2.02

[a] See Figures 1 and 2 for clusters and oxygen labels. For smaller cluster models, only bond lengths to *hydrogenated* oxygen atoms are available; such bonds are ignored in larger models where internal oxygen atoms do occur. [b] Bonds in cluster center. [c] Bonds next to cluster center. [d] Crystallographic data from ref 34.

constraints mentioned above. A comparison of some of the geometrical parameters (V−V and V−O distances) from the optimized and crystallographic structures are given in Table 1. The results indicate that most of the optimized distances in the cluster are close to those in the crystal structure. Transition states were located using standard conjugate-gradient methods in the Gaussian codes.[33] Because of difficulties locating the transition states for the dissociative adsorption of propane on the V_2O_5 surface using standard conjugate-gradient techniques, in some cases they were located via the nudged elastic band method.[37,38]

b. Periodic Calculations. Periodic calculations on certain equilibrium structures were carried out to test the validity of the cluster calculations. The periodic density functional calculations were performed using the CRYSTAL03 program.[34] Bulk V_2O_5 is an orthorhombic crystal with a space group $Pmn2_1$ and lattice parameters $a = 11.51$ Å, $b = 4.37$ Å, and $c = 3.56$ Å.[35] Each unit cell contains two V_2O_5 units. The crystal is composed of slabs of six planar atomic layers (four oxygen layers and two vanadium layers) with the normal direction along (010) as shown in Figure 1. We used (1 × 2) and (1 × 3) supercells of (010) single slabs to model the surfaces. To model the equilibrium structures, the optimized geometries obtained using the **V4** cluster were embedded (without hydrogen atoms) in these periodic surface models such that the unrelaxed atoms of the cluster matched the corresponding lattice positions. To calculate the adsorption energy, single point energy calculations were performed on periodic models of (1 × 2) and (1 × 3) bare surfaces and an isolated fully optimized propane molecule. These calculations used the B3PW91 density functional and 6-31G-(*) basis set. The integrations over the irreducible Brillouin zone were performed using the Monkhorst−Pack method[39] with sets of 10 and 4 *k*-points for (1 × 2) and (1 × 3) surfaces, respectively. The integration tolerances and grids were set to exactly reproduce single-point total energies of cluster calculations described in section 2a when the same geometry is used.

3. Results and Discussion

a. Geometries and Energies. We investigated the reaction of propane with the vanadyl and bridging oxygen sites of the (010) V_2O_5 surface. These correspond to the O(1) and O(2) sites in Figure 1, respectively. The O(3) bridging site is also a possibility, but we found it to be a less likely site for the propane reaction due to steric hindrances. The reactions on the O(1) vanadyl site were studied with clusters **V1**, **V2**, **V4**, and **V10−B** shown in Figure 2. Most of the calculations were done with the **V4** cluster, $V_4O_{14}H_8$, and the other three clusters were used to study the convergence of relative energies with cluster size. The reactions on the O(2) bridging oxygen site were investigated using the **V6** cluster, $V_6O_{23}H_{16}$, shown in Figure 2. The **V10-A** cluster (an inverted **V10-B** cluster) was also used to model the O(2) site.

The singlet equilibrium structures that were investigated for propane ODH to form propene and water are shown in Figure 3. The species in the reaction at the vanadyl site [O(1)] include (1) the reactants: propane, O_2, and the **V4** cluster, (2) a propanol adsorbate structure resulting from insertion of a vanadyl oxygen into a secondary C−H bond of propane, **V4(propanol)**, (3) a propoxide adsorbate structure resulting from hydrogen migration from the adsorbed propanol to a neighboring vanadyl oxygen, **V4(propoxide, OH)**, (4) either of two structures having a pair of OH groups after desorption of propene, **V4(OH,OH)**$_{adjacent}$ and **V4(OH,OH)**$_{opposite}$, (5) a structure resulting from hydrogen migration from an OH to a neighboring OH, **V4(H$_2$O)**, (6) a cluster with an oxygen vacancy resulting from desorption of water, **V4(O$_{vacancy}$)** and (7) the products: propene, water and the **V4** cluster. The structures for species (2)−(6) are shown in Figure 3 and the relative B3LYP/6-31G(*) energies for all minima are given in Table 2. For the reaction initiated at the O(2) bridging site, we investigated the formation of a propoxide adsorbate structure resulting from dissociative adsorption of propane via breaking of a secondary C−H bond, **V6(propoxide, OH)**, which is shown in Figure 3. The subsequent energy minima in the reaction sequence initiated at the O(2) site are assumed to be similar to those initiated at the vanadyl site, and thus we have not included any energies in this sequence. The relative B3LYP/6-31G(*) energies for reaction at the bridging O(2) site are given in Table 2. We also investigated reaction of a terminal C−H bond in propane with the vanadyl site and found it to be less favorable by 4 kcal/mol and did not consider it further in this study.

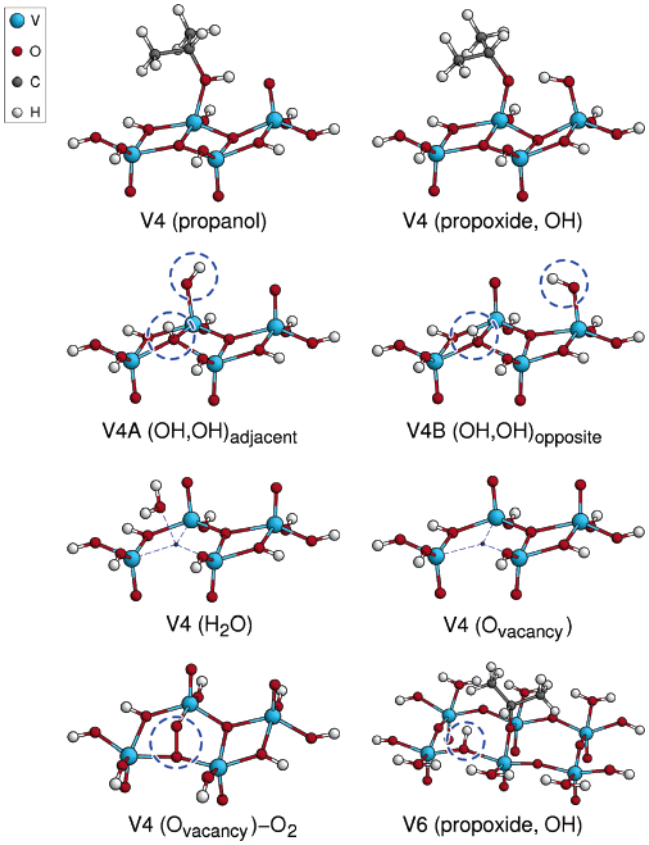

Figure 3. Structures of energy minima on the ODH reaction pathways from calculations on **V4** and **V6** clusters.

The neutral oxygen vacancy may be a singlet or a triplet. Thus, we considered a triplet configuration for the **V4(O$_{vacancy}$)** structures. In addition, the other energy minima resulting from propane insertion may have unpaired electrons due to the bond breaking. Thus, we also considered the possibility that the other structures in the reaction scheme may be in a triplet configuration. The geometries of all of the structures described above were also optimized as a triplet state using B3LYP/6-31G(*). The relative energies of the triplet states are given in Table 2. In most cases the geometries did not change significantly, except where noted in the following discussion. The singlet−triplet energy difference of 47−53 kcal/mol for the V_2O_5 cluster models in Table 2 is consistent with the experimental band gap of about 2.2 eV (51 kcal/mol) of V_2O_5.

Finally, transition state structures were located for the propane reaction at the vanadyl site and the bridging oxygen site for all of the steps in the reaction mechanisms. This was done initially for the singlet states, and then these optimized geometries were used for single-point calculations for the triplet state. We investigated the uncertainty introduced by the use of the singlet transition state geometry for calculating the triplet state energy in one case and found that the barrier was too high by about 6 kcal/mol compared to a full optimization of the transition state. Based on this, we have assumed that this approximation will introduce only small uncertainties in the triplet state barriers. The energies of the singlet and triplet transition states relative to the reactants for both pathways are listed in Table 3.

b. Reaction at the Vanadyl Oxygen Site. The reaction pathway investigated for the reaction of propane and O_2 on a V_2O_5 surface initiated at the vanadyl site is illustrated in Figure 4. This pathway has barriers that are in the range 79−91 kcal/mol for the $V_4O_{14}H_8$ cluster model and singlet state configurations. The barriers are reduced when the possibility of a singlet/triplet crossing is included. The energies of the steps in this pathway including both singlet and triplet configurations are described below.

The first barrier (**TS 1→2**), which is 79.4 kcal/mol, corresponds to insertion of the vanadyl oxygen into a secondary C−H bond to form the **V4(propanol)** structure. The formation of the **V4(propanol)** structure is endothermic by 32.6 kcal/mol. We confirmed the endothermicity of this step through a cluster size (**V1**, **V2**, **V4**, **V10-B**) dependence study and periodic calculations. These results, which are listed in Table 4, indicate that formation of the propanol structure is endothermic by 25.9 kcal/mol with the **V10-B** cluster and 26.8 kcal/mol with the periodic calculations. The results in Table 2 indicate that the triplet state **V4(propanol)** structure is significantly lower in energy than the singlet, its formation being endothermic by only 6.6 kcal/mol with respect to the ground-state reactants. Results (see Table 4) for a larger **V10-B** cluster (1.8 kcal/mol) and the periodic model (2.1 kcal/mol) also confirmed this result. Thus, the triplet state of **V4(propanol)** is more stable than the singlet by about 25 kcal/mol. We investigated the barrier to reach the triplet state **V4(propanol)** structure from the reaction of propane with the **V4** cluster in the triplet state and found the insertion on this triplet surface to be much easier with a barrier of only 6.4 kcal/mol. Thus, the triplet transition state is 55.0 kcal/mol above the initial reactants based on a singlet state **V4** cluster as indicated in the reaction scheme in Figure 4. We investigated a triplet/singlet surface crossing for propane insertion using the **V2** cluster and the nudged elastic band method.[37,38] We found that the transition state structure for the triplet surface is about the same as the transition state for the minimum energy path connecting the singlet **V2** reactant and the triplet propanol-**V2** adsorbate. This indicates that the barrier for propane insertion would be significantly reduced (from 79.4 to 55.0 kcal/mol) by a triplet/singlet surface crossing.

A Mulliken analysis of the **V4(propanol)** wave function indicates that there is charge transfer to the vanadium and oxygen atoms on the surface due to the breaking of the V═O double bond and that in the triplet state the two unpaired electrons are largely localized on the vanadium to which the propanol is attached. Thus, the vanadium is partially reduced in the propanol adsorbate structure, which is the reason the triplet state is lower in energy than the singlet. Likewise, the triplet is more stable than the singlet for the other adsorbate and transition state structures in subsequent steps (see below) in the reaction pathway. The energy lowering of the triplet state of the propanol adsorbate predicted by B3LYP/6-31G(*) was investigated and confirmed by a CCSD(T) calculation, which is more reliable than B3LYP for singlet/triplet energy differences. A CCSD(T)/6-31G* calculation on the VO_5H_5 cluster with a propanol adsorbate predicts the triplet to be 31.1 kcal/mol lower in energy than the singlet, in reasonable agreement with the energy difference of 26.0 kcal/mol (Table 4) predicted by B3LYP/6-31G(*).

Two paths were considered for desorption of propene from the **V4(propanol)** structure. The first involves hydrogen migration (**TS 2→3**) to the adjacent vanadyl oxygen to form the **V4(propoxide,OH)** structure shown in Figure 3. This migration has a small barrier of only 9.7 kcal/mol and is followed by hydrogen migration (**TS 3→4B**) from a terminal CH_3 group of propane to an O(3) oxygen [**V4(OH,OH)**$_{opposite}$ in Figure 3]. This migration has a barrier of 41.2 kcal/mol relative to **V4(propanol)** (or 83.5 kcal/mol relative to the reactants). The second path (**TS 2→4A**) involves only a single hydrogen migration, i.e., from a terminal CH_3 group on the propanol adsorbate to the same O(3) oxygen adjacent to the OH

TABLE 2: Relative Energies (in kcal/mol) of Energy Minima on the Reaction Pathway for Propane Reacting with a Vanadyl Oxygen Site [O(1)] on a $V_4O_{14}H_8$ (V4) Cluster and a Bridging Oxygen Site [O(2)] on a $V_6O_{23}H_{16}$ (V6) Cluster

	B3LYP/6-31G*		B3LYP/G3MP2Large[a]	
energy minima	singlet[b]	triplet[b]	singlet[b]	triplet[b]
	Reaction at O(1)			
1. **V4** + C_3H_8 +1/2O_2	0.0	48.6	0.0	52.7
2. **V4(propanol)** +1/2 O_2	32.6	6.6	32.1	8.0
3. **V4(propoxide,OH)** +1/2O_2	42.3	11.1	42.2	10.7
4. **V4(OH,OH)** + C_3H_6 +1/2O_2	65.9[c], 67.7[d]	32.3	56.7[c], 60.9[d]	25.2
5. **V4(H_2O)** + C_3H_6 +1/2O_2	78.9	52.3	70.6	48.3
6. **V4($O_{vacancy}$)** + C_3H_6 + H_2O+1/2O_2	90.7	80.5	74.0	65.2
7. **V4** + C_3H_6 + H_2O	−7.7	40.9	−24.1	28.6
	Reaction at O(2)			
1. **V6** + C_3H_8 + 1/2O_2	0.0	47.2	0.0	51.7
2. **V6(propoxide,OH)** +1/2O_2	30.5	1.3	41.0	11.5

[a] At the B3LYP/6-31G(*) geometry. See Figure 3 for illustration of singlet structures. [b] Singlet or triplet refers to the electronic configuration of the **V4** (or **V6**) cluster and adsorbate (if any). H_2O, C_3H_8, and C_3H_6 are $^1A_1$ and O_2 is in the $^3\Pi$ state. The energies are all relative to **V4** (singlet) [or **V6** (singlet)] + $C_3H_8(^1A_1)$ + 1/2$O_2(^3\Pi)$. [c] Result for structure **4A** (see Figure 3) with OH groups in adjacent positions. [d] Results for structure **4B** (see Figure 3) with OH groups in opposite positions.

TABLE 3: Energy Barriers[a](in kcal/mol) in the Reaction Pathway for Propane Reacting with a Vanadyl Oxygen on a $V_4O_{14}H_8$ (V4) Cluster and with a Bridging Oxygen on a $V_6O_{23}H_{16}$ (V6)[b]

transition state	state	B3LYP/6-31G(*) singlet	B3LYP/6-31G(*) triplet[d]	B3LYP/G3MP2Large[c] singlet	B3LYP/G3MP2Large[c] triplet[d]
		Reaction at O(1)			
TS(1 → 2)	singlet	79.4	[55.0]	76.8	[53.6]
TS(2 → 3)	singlet	42.3	[27.3]	42.2	[23.4]
TS(2 → 4A)	singlet	81.3	[59.4]	80.3	[58.8]
TS(3 → 4B)	singlet	83.5	[60.3]	82.5	[59.5]
TS(4A → 5)	singlet	87.8	[76.3]	81.7	[71.8]
		Reaction at O(2)			
TS(1 → 2)	singlet	59.7	[45.2]		

[a] All barriers are relative to **V4**(singlet) [or **V6**(singlet)] + $C_3H_8(^1A_1)$+ 1/2$O_2(^3\Pi)$. [b] Numbers refer to Table 2 entries. Values in square brackets are from single point calculations at the singlet transition state geometries. [c] At the B3LYP/6-31G* geometry. [d] The triplet energies correspond to the transition state structures of the **V4** (or **V6**) cluster with an adsorbate in the lowest energy triplet configuration.

group, which results in desorption of propene and the **V4-(OH,OH)**$_{adjacent}$ structure shown in Figure 3. This step has a barrier of 48.7 kcal/mol relative to **V4(propanol)** (and 81.3 kcal/mol relative to the reactants). Thus, both steps have similar barriers and the resulting structures [(**V4(OH,OH)**$_{opposite}$ and **V4(OH,OH)**$_{adjacent}$)] are about 66 kcal/mol higher in energy than the reactants. The two reaction paths were also investigated for the triplet states, and the stationary points on the surface were found to lie 20−30 kcal/mol lower in energy than the singlets (see Tables 2 and 3, Figure 4). This is similar to the results for the propanol adsorbate that gave a lower energy for the triplet state, although in this case two nearby vanadium sites each have an unpaired electron.

Next we investigated migration of a hydrogen from an OH group to a neighboring OH group to form a surface-bound water molecule (**4A→5**). This migration has a barrier of 21.9 kcal/mol (87.8 kcal/mol relative to the reactants). The resulting equilibrium structure [**V4(H_2O)**] at the O(3) site corresponds approximately to a water loosely bound to the surface (with one V−O bond of about 2.2 Å) as shown in Figure 3. It is located 78.9 kcal/mol above the reactants. When this structure is optimized in the triplet configuration, the water unit is more strongly bound to the surface and is located 52.3 kcal/mol above the singlet state reactants. This is reflected in the formation of a second V−O bond in the triplet **V4(H_2O)** structure, which is not present in the singlet.

The next step involves desorption of the water molecule from the surface, which leaves an oxygen vacancy on the surface at an O(3) site, **V4($O_{vacancy}$)**. This structure corresponds to the highest energy on the potential energy surface. It is 90.7 kcal/mol higher in energy than the reactants and we found no barrier for the desorption of H_2O other than the energy by which it is bound to the surface (11.8 kcal/mol). The triplet state **V4-($O_{vacancy}$)** structure is located 80.5 kcal/mol above the singlet state reactants. The desorption of water from the triplet configuration requires 28.3 kcal/mol. Since the oxygen vacancy has the highest energy on the pathway, we investigated its energies with the larger **V6** and **V10** clusters. The results are given in Table 4 and the relative energies are consistent with what was found for the **V4** cluster, although the dependence on cluster size is more significant for the triplet state and the singlet and triplet configurations are similar in energy for the **V10** cluster (about 95 kcal/mol above the reactants).

Finally, we investigated the addition of oxygen to a vacancy to regenerate the oxide surface. This was done by considering a **V4** cluster with an oxygen vacancy at the O(3) site shown in Figure 3 and optimizing a structure with O_2 added to the vacancy [**V4($O_{vacancy}$)**-O_2 in Figure 3]. Key energies related to filling the vacancy are given in Table 5: (1) an adsorbed O_2 at the vacancy, (2) a "filled" vacancy cluster [**V4**] plus a free oxygen atom, and (3) the final product, i.e., a "filled" vacancy cluster [**V4**] plus 1/2O_2. These results correspond to filling of the oxygen vacancy, without consideration of barriers for oxygen dissociation or diffusion of an oxygen. Assuming that the barriers are small, the results indicate that filling the oxygen vacancy is energetically downhill with an energy for O_2 binding in the vacancy of 55 kcal/mol (relative to the triplet vacancy) and 88.2 kcal/mol for going to the filled vacancy plus 1/2O_2, which is equivalent to the final point on the pathway.

Thus, the multistep reaction pathway for the ODH reaction of propane and O_2 initiated at the vanadyl site has a maximum energy of 80.5 kcal/mol (above the reactants) if one includes the possibility of singlet/triplet surface crossings based on the **V4** cluster results in Table 2. The overall reaction is exothermic by 7.7 kcal/mol. The highest energy on the surface corresponds to the oxygen vacancy structure.

We also calculated B3LYP single point energies with the larger G3MP2Large basis set, which was described in section 2, for the reaction pathway initiated at the O(1) site. These energies are given in Tables 2 and 3. The use of a larger basis set had some effect on barriers (<6 kcal/mol) and relative

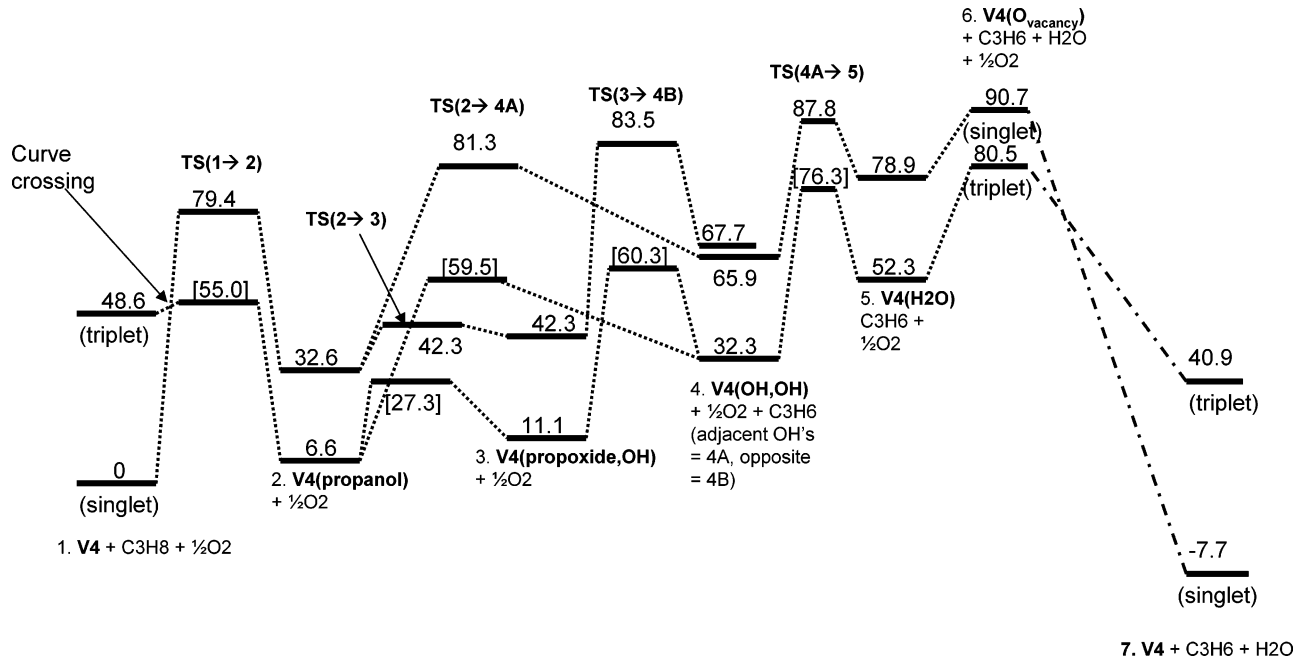

Figure 4. Illustration of the singlet and triplet reaction pathways for ODH at the O(1) vanadyl site based on B3LYP/6-31G(*) calculations on the $V_4O_{14}H_8$ (**V4**) cluster [energies are in kcal/mol and all are relative to the **V4** cluster (singlet) + C_3H_8 ($^1A_1$) + 1/2O_2 ($^3\Pi$); structures of singlet energy minima shown in Figure 3; values in square brackets are from single point calculations at the singlet transition state geometries.]

TABLE 4: Comparison of Energies[a] (in kcal/mol) of Different Size Clusters[b] and the Periodic Model for Propane Reaction at the Vanadyl and Bridging Oxygen Sites

		B3LYP/6-31G(*)					B3PW91/6-31G(*)
energy minimum	state	V1	V2	V4	V6	**V10**[c]	periodic[d]
			Reaction at O(1)				
1. **Vn** + C_3H_8 +1/2O_2	singlet	0.0	0.0	0.0		0.0	0.0
2. **Vn(propanol)** + 1/2O_2	singlet	53.0	39.1	32.6 (35.0)[e]		25.9[f]	26.8
	triplet	27.0	12.5	6.6		1.8[f]	2.1
3. **Vn(propoxide,OH)** +1/2O_2	singlet		47.8	42.3 (44.5)[e]			35.0
	triplet			11.1			5.6
6. **Vn($O_{vacancy}$)** + C_3H_6 + H_2O+1/2O_2	singlet			90.7	93.6	94.2	
	triplet			80.5	72.2[f]	96.0[g]	
			Reaction at O(2)				
1. **Vn** + C_3H_8 +1/2O_2	singlet				0.0	0.0	0.0
2. **Vn(propoxide)** + 1/2O_2	singlet				30.2	35.7	41.2
	triplet				1.3	5.7	13.2

[a] The energies reported in the table are all relative to **Vn**(singlet) + C_3H_8($^1A_1$) + 1/2O_2($^3\Pi$). The periodic results are relative to the closed shell surface + C_3H_8($^1A_1$) + 1/2O_2($^3\Pi$). [b] **V1** = $V_1O_5H_4$, **V2** = $V_2O_9H_8$, **V4** = $V_4O_{14}H_8$, **V6**=$V_6O_{23}H_{16}$, **V10** = $V_{10}O_{31}H_{12}$. Periodic refers to (3 × 1) supershell. See Figure 2 for illustration of structures. [c] Optimized result except where noted. The O(1) reaction uses **V10-B** and the O(2) reaction uses **V10-A**. (see Figure 2). [d] Single point calculations at the B3LYP geometry from **V4** cluster (O(1) reaction pathway) and **V6** cluster (O(2) reaction pathways). [e] Values in parentheses are from B3PW91/6-31G* calculations. [f] Geometry taken from **V4** (embedded in the **V10** cluster). [g] Vanadyl oxygens below the surface in **V6** and **V10-B** held frozen in the optimizations of the vacancy structure.

TABLE 5: Relative Energies (in kcal/mol) of Equilibrium Structures for Filling an Oxygen Vacancy in a $V_4O_{14}H_8$ (V4) Cluster by O_2

	B3LYP/6-31G(*)	B3LYP/G3MP2Large[a]
V4($O_{vacancy}$)[b]+ O_2($^3\Pi$)	0.0	0.0
V4($O_{vacancy}$)-O_2[c]	−54.6	−52.2
V4[c] + O(^{3}P)	−25.8	−27.7
V4[c] + 1/2O_2($^3\Pi$)	−88.2	−87.5

[a] At the B3LYP/6-31G(*) geometry. [b] Triplet state. [c] Singlet state.

energies (<17 kcal/mol). The overall reaction energy for the oxidative dehydrogenation of propane becomes −24.1 kcal/mol (at 0 K), which compares well to the experimental value of −27.3 kcal (at 298 K). The highest triplet energy on the surface based on the large basis set calculation is for the transition state structure **TS(4A→5)**, which corresponds to migration of a hydrogen from an OH group to a neighboring OH group and has an energy of 71.8 kcal/mol above the reactants. However, the larger basis set results do not change the overall picture of the potential energy surface of large barriers and endothermic reactions for all steps in the mechanism until the last step.

c. Reaction at the Bridging Oxygen Site. The pathway for the reaction of propane and O_2 on a (010) V_2O_5 surface that is initiated at the bridging O(2) oxygen site is assumed to be very similar to that of the vanadyl site with the exception of the first step, in which propane is dissociatively adsorbed onto the bridging oxygen site instead of the vanadyl site. The energetics for hydrogen migration to eliminate water and create a vacancy should be similar since it will occur at the O(3) site. Thus, we have only done calculations on this first step to find out how it compares energetically with the reaction at the vanadyl site. The results are given in Tables II, III, and IV and illustrated in Figure 5. The **V6** cluster (Figure 2) was used in this investigation. The barrier for dissociative adsorption of propane at the

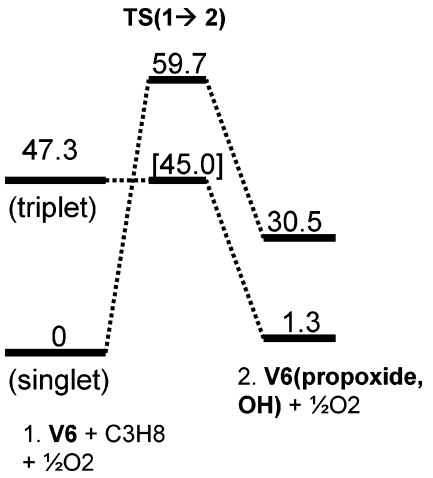

Figure 5. Illustration of the singlet and triplet reaction pathways for propane addition at the O(2) bridging oxygen site based on B3LYP/6-31G(*) calculations on the $V_6O_{23}H_{16}$ (**V6**) cluster [energies are in kcal/mol and all are relative to the **V6** cluster (singlet) + C_3H_8 ($^1A_1$) + 1/2O_2 ($^3\Pi$); structure of singlet energy minimum shown in Figure 3; value in square brackets is from single point calculations at the singlet transition state geometry.]

bridging site **TS(1→2)** is 59.7 kcal/mol, which is about 20 kcal/mol less than the barrier of 79.4 kcal/mol for the O(1) pathway. The barrier involves interaction of propane at the O(2) site that results in breaking a secondary C−H bond followed by formation of propoxide at a O(2) site and an OH group at a O(3) site (**V6(propoxide,OH)** in Figure 3). The formation of the **V6(propoxide,OH)** structure is endothermic by 30.5 kcal/mol. The results from the **V10-A** cluster (see Table 4) indicate that the formation of the propoxide structure is endothermic by 35.7 kcal/mol and the periodic model indicates that it is endothermic by 41.2 kcal/mol. The energies are similar to the **V4(propoxide,OH)** propoxide structure on the O(1) pathway, which is endothermic by 42.3 kcal/mol for the **V4** cluster and 35.0 kcal/mol for the periodic model.

The triplet state pathway has little or no barrier for breaking of the C−H bond at the O(2) site as the transition state has approximately the same energy as the triplet **V6** cluster plus reactants (see Tables 2 and 3). Thus, a singlet/triplet surface crossing gives an overall barrier of about 45 kcal/mol (see Figure 5), which is about 10 kcal/mol less than that of the O(1) pathway. The resulting **V6(propoxide,OH)** structure is significantly lower in energy as a triplet than the singlet for reasons similar to those discussed above for the vanadyl site. Its formation is endothermic by 1.3 kcal/mol compared to 30.5 kcal/mol for the singlet structure. The Mulliken spin densities are located on the two vanadiums nearest the propoxide. Although the barrier is slightly lower, the energetics at the O(2) site, within the uncertainties of our calculation, are quite similar to what we found for the reaction at the O(1) site. We conclude that the energetics for propane ODH on the bridging and vanadyl oxygens on the (010) V_2O_5 surface are probably quite similar.

d. Other Theoretical Studies. There have been a number of quantum chemical studies of vanadium oxide surfaces, but only one paper has dealt with propane adsorption. Gilardoni et al.[21] examined propane ODH on a vanadium oxide surface using the BPW91 density functional method, a mixed basis set, and cluster models of the (010) V_2O_5 surface. They found that the initial step in the dissociative adsorption of propane to form i-propoxide and hydroxide species involved two V═O groups. One of the V═O groups attacked a β-C atom of propane and was converted to a V−OCH$(CH_3)_2$ propoxide species, while the other V═O group formed a V−OH species. This step was reported to be *exothermic* by 36.4 kcal/mol (singlet configuration) while the same step calculated using our **V2** cluster is *endothermic* by 39.1 kcal/mol (Table 4). Gilardoni et al. assigned an energy barrier of 9.4 kcal/mol to this process, corresponding to the transition state for migration of the hydrogen to the second V═O group. No transition state for the initial attack of propane on the vanadyl oxygen was identified. Gilardoni et al.[21] also investigated a subsequent step in the ODH sequence that led to the formation of propene and water involving abstraction of a methyl hydrogen from the i-propoxide. This was found to have a barrier of about 15 kcal/mol. Thus, results reported by Gilardoni et al. are in disagreement with our results, which indicate that the dissociative adsorption of propane at the vanadyl oxygen is endothermic with a large barrier and that the subsequent steps are also endothermic with large barriers.

The reason for the difference in the dissociative adsorption is because Gilardoni et al. used a two vanadium atom cluster ($V_2O_9H_6$) with six terminal OH groups, while our **V2** cluster ($V_2O_9H_8$) has four terminal OH groups and two terminal OH_2 groups. As described in section 2, the termination used in **V2** accurately represents the bonding situation on the V_2O_5 surface and corresponds to vanadium and oxygen in formal valence states of +5 and −2. By contrast, the use of Mulliken population analysis shows that the OH termination in the $V_2O_9H_6$ cluster corresponds to the OH oxygens in a partially oxidized state, which probably explains why this cluster is more reactive. The endothermicity of the propane reaction on the (010) surface is confirmed by the results for the **V4** cluster, which does not require the termination by OH_2 groups (see Figure 2, Table 2). It is further confirmed by the periodic results (Table 4), which also indicate that the dissociative adsorption of propane is endothermic.

The oxygen vacancy plays an important role in the reaction pathway studied here since the step that involves its formation has the highest energy on the potential energy surface. There have been a number of theoretical studies of the oxygen vacancies on a clean V_2O_5 surface. Lambrecht et al.[19] calculated electronic states of a vanadyl vacancy in a single layer periodic model using a tight-binding method. They suggested on the basis of a two-level model that a triplet state is more energetically favorable than a singlet. Hermann et al.[13,20] have studied surface oxygen vacancies in one and two layer cluster models ($V_{10}O_{31}H_{12}$ and $V_{20}O_{62}H_{24}$) using density functional methods, with no mention of the spin state. All three oxygen sites were considered, O(1), O(2), and O(3). They calculate an oxygen vacancy energy of 150 kcal/mol for removal of an oxygen atom from the O(3) site for their single layer model and about 140 kcal/mol for their double-layer model. Ganduglia−Pirovano and Sauer[18] reported calculations of total energy and electronic structure of surface vacancies in V_2O_5 as a function of their surface concentration using spin-unrestricted density functional theory and a double layer periodic model. They found the ground state of the vacancy to be a triplet and the energy for O atom removal from the O(3) site to be about 163 kcal/mol at 1/6 monolayer coverage. Our value of 164 kcal/mol (singlet) and 166 kcal/mol (triplet) from the single-layer **V10-B** cluster at the B3LYP/6-31G(*) level is consistent with the previous studies, although we note that there is a 20 kcal/mol variation between the previous results. In addition, Tokarz-Sobieraj et al.[40] have recently investigated the interaction of O_2 with vacancies on a (010) V_2O_5 surface and found O_2 adsorption to be an exothermic process consistent with our results.

It is also relevant to note that a previous experimental and computational study of propane ODH via reaction with the VO_2^+

molecular ion has given evidence for a crossing point between singlet and triplet potential energy surfaces.[41] Although the reaction mechanism is somewhat different than the one investigated in the current work, it suggests that vanadium oxide systems can exhibit so-called "two-state reactivity"[42] in alkane ODH reactions, which is what we report here. Also, a recent study of oxidation of methanol to formaldehyde on a supported vanadium oxide catalyst has found intermediates to have a lower energy as a triplet state.[43]

e. Comparison to Experiment. Several recent experimental results have contrasted the catalytic properties of pure V_2O_5 and supported vanadia catalysts for methanol oxidation and ODH of propane. Utilizing a variety of spectroscopic techniques, Wachs et al.[44] conclude that the active sites for oxidation reactions are found *at the edges* of bulk V_2O_5 platelets and *not* on the (010) basal planes. This is reflected in a surface density of active sites for supported vanadia catalysts (i.e., V_2O_5/TiO_2) that is twenty times larger than for bulk V_2O_5. This is consistent with the results of our calculations giving large barriers for the reaction of propane on the (010) surface of V_2O_5.

The experimental barriers for propane ODH on supported vanadium oxide are in the range 20−30 kcal/mol,[4,10,22] which are much lower than the value of about 80 kcal/mol found in this study for the water elimination step. The calculated barriers for the steps preceding water elimination are also significantly larger than experiment. There are a number of scenarios that could reduce the barriers for the water elimination steps (4→5 and 5→6) and we discuss three of them here. First, instead of the stepwise reaction path we have considered, it is possible that a concerted reaction, involving the participation of an adsorbed O_2 molecule, could reduce the barriers for the water elimination steps. This is suggested by our result that shows a large energy stabilization of about 50 kcal/mol when O_2 is adsorbed at an oxygen vacancy site. This possibility is consistent with the methanol oxidation results of Boulet et al.[26] described earlier. Second, we found in the case of the triplet state that the vanadyl oxygens that point down (under the surface) will bend to fill the vacancy being created by the oxygen leaving the surface. In the calculations reported in Tables 2 and 3 for this step, we have frozen these vandyls because of the lack of a second layer of V_2O_5. Both the concerted reaction and relaxation of the downward pointing vandyl oxygens require a more detailed study, but are possible mechanisms by which the water elimination barrier can be significantly lower than shown in Figure 4. Third, our study has been based only on water elimination from the O(3) site, but it is possible that reaction pathways through the O(1) or O(2) sites may be lower in energy. Based on the vacancy energies reported by Hermann et al.[13] this is not likely as the O(1) vacancy has the same oxygen removal energy as the O(3) site and the O(2) vacancy has a higher energy. In contrast, Ganduglia-Pirovano and Sauer[18] in their more thorough periodic study find that it is significantly easier (by 15−40 kcal depending on geometry relaxation) to remove the oxygen from the vanadyl oxygen site, O(1), than the O(3) site. If oxygen elimination is easier at the O(1) than the O(3) site, this could also significantly reduce the barriers for the water elimination. All of the scenarios described above require further study for a complete picture of ODH on the V_2O_5 surface, but the preliminary indications suggest that the barriers for water elimination steps (4→5 and 5→6) will not be nearly as large as in the reaction pathway in Figure 4.

Even if the barriers in the water elimination steps are lower due to one or more of the scenarios described above, the barriers for the initial dissociative adsorption and the propene elimination step (45−60 kcal/mol) are still much higher than found experimentally, even on the triplet pathway. Thus, assuming that the approximations used in our computations are valid, these results suggest that propane ODH on supported vanadium oxide species differs from that on a clean (010) V_2O_5 surface.

Our results point toward a possible reason as to why the interaction of vanadium oxide with a support may lower the barrier for the initial dissociative adsorption of propane and propene elimination steps in the ODH reaction pathways investigated here, although at this point it remains somewhat speculative. Analogous to the stabilization of the triplet state relative to the singlet state when the vanadium oxide surface is reduced by adsorbates (e.g., propanol, propoxide, and OH in Tables 2 and 4), the triplet state of a vanadium oxide cluster may be stabilized relative to the singlet (though not necessarily lower in energy) if anchored such that it is in a reduced state on a support. If true, this effect would stabilize the triplet stationary points on the potential surface with respect to the reactants all along the reaction path, and a lower overall barrier would result. We are currently investigating this possibility in more detail, and results for supported catalytic sites will be reported in the future.

4. Conclusions

The following conclusions can be drawn from this B3LYP/6-31G(*) density functional study of a Mars-van Krevelen mechanism for ODH of propane on the (010) surface of V_2O_5 using both vanadium oxide clusters and a periodic slab model.

1. The potential energy surface is found to have large barriers, which are lowered somewhat when the possibility of a triplet state is considered. The triplet state is stabilized by breaking of surface bonds by adsorbates and transfer of charge to the surface. The reaction at a V−O−V bridging oxygen site is energetically similar to that at a V═O vanadyl site.

2. The barriers on the reaction pathway are 45−80 kcal/mol above the energy of the reactants, which are much larger than found experimentally for propane ODH on supported vanadia. The highest energy on the reaction pathway of 80 kcal/mol corresponds to an oxygen vacancy at the O(3) site on the V_2O_5 surface, which forms when a water molecule is desorbed. The barriers for propane adsorption and propene elimination are also large (45−60 kcal/mol).

3. Some of the barriers may be reduced by consideration of more complex reactions, such as a concerted reaction involving adsorption of O_2 during water elimination. The reduction of other barriers, such as for propane adsorption, appear to require the involvement of a support for the vanadium oxide catalyst.

Acknowledgment. This work was supported by the Office of Basic Energy Sciences, U.S. Department of Energy, under Contract No. W-31-109-ENG-38. We acknowledge computational resources from the Argonne National Laboratory − Laboratory Computing Resource Center and the U.S. Department of Energy National Energy Research Scientific Computing Center.

References and Notes

(1) Cavani, F.; Trifiro, F. *Catal. Today* **1995**, *24*, 307.

(2) Ruitenbeek, M.; van Dillen, A. J.; de Groot, F. M. F.; Wachs, I. E.; Geus, J. W.; Konigsberger, D. C. *Top. Catal.* **2000**, *10*, 241.

(3) Izumi, Y.; Kiyotaki, F.; Yoshitake, H.; Aika, K.; Sugihara, T.; Tatsumi, T.; Tanizawa, Y.; Shido, T.; Iwasawa, Y. *Chem. Commun.* **2002**, 2402.

(4) Argyle, M. D.; Chen, K.; Bell, A. T.; Iglesia, E. *J. Catal.* **2002**, *208*, 139.

(5) Ferreira, M. L.; Volpe, M. *J. Mol. Catal.* A **2002**, *184*, 349.

(6) Gao, X.; Jehng, J.; Wachs, I. E. *J. Catal.* **2002**, *209*, 43.
(7) Mars, P.; van Krevelen, D. W. *Chem. Eng. Sci.* **1954**, *3*, 41.
(8) Oyama, S. T. *J. Catal.* **1991**, *128*, 210.
(9) Eon, J. G.; Olier, R.; Volta, J. C. *J. Catal.* **1994**, *145*, 318.
(10) Chen, K.; Bell, A. T.; Iglesia, E. *J. Phys. Chem. B* **2000**, *104*, 1292.
(11) Weckhuysen, B. M.; Keller, D. E. *Catal. Today* **2003**, *78*, 25.
(12) Witko, M.; Tokarz, R.; Haber, J. *Appl. Catal.* A **1997**, *157*, 23.
(13) Hermann, K.; Witko, M.; Druzinic, R.; Tokarz, R. *Appl. Phys. A* **2001**, *72*, 429.
(14) Kachurovskaya, N. A.; Mikheeva, E. P.; Zhidomirov, G. M. *J. Mol. Catal. A* **2002**, *178*, 191.
(15) Calatayud, M.; Mguig, B.; Minot, C. *Surf. Sci.* **2003**, *526*, 297.
(16) Vittadini, A.; Selloni, A. *J. Phys. Chem. B* **2004**, *108*, 7337.
(17) Brazdova, V.; Ganduglia-Pirovano, M. V.; Sauer, J. *Phys. Rev. B* **2004**, *69*, 165420.
(18) Ganduglia-Pirovano, M. V.; Sauer, J. *Phys. Rev. B* **2004**, *70*, 045422.
(19) Lambrecht, W.; Djafari-Rouhani, B.; Vennik, J. *Solid State Commun.* **1981**, *39*, 257.
(20) Hermann, K.; Witko, M.; R. Druzinic, R. *Faraday Discuss.* **1999**, *114*, 53.
(21) Gilardoni, F.; Bell, A. T.; Chakraborty, A.; Boulet, P. *J. Phys. Chem. B* **2000**, *104*, 12250.
(22) Heracleous, E.; Machli, M.; Lemonidou, A.; Vasalos, I *J. Mol. Catal.* **2005**, *232*, 29.
(23) Fu, G.; Xu, X.; Wan, H. *J. Phys. Chem. B* **2005**, *109*, 6416.
(24) Haber, J.; Witko, M. *J. Catalysis* **2003**, *216*, 416.
(25) Khaliullin, R. Z.; Bell, A. T. *J. Phys. Chem. B* **2002**, *106*, 7832.
(26) Boulet, P.; Baiker, A.; Chermette, H.; Gilardoni, F.; Volta, J.-C.; Weber, J. *J. Phys. Chem.* B **2002**, *106*, 9659.
(27) Becke, A. D. *J. Chem. Phys.* **1993**, *98*, 5648. Stephens, P. J.; Devlin, F. J.; Chabalowski, C. F.; Frisch, M. J. *J. Phys. Chem.* **1994**, *98*, 11623.
(28) Curtiss, L. A.; Raghavachari, K.; Redfern, P. C.; Pople, J. A. *J. Chem. Phys.* **1997**, *106*, 1063.
(29) Curtiss, L. A.; Redfern, P. C.; Raghavachari, K. *J. Chem. Phys.* **2005**, 124107 2005.
(30) Rassolov, V.; Pople, J. A.; Ratner, M.; Redfern, P. C.; Curtiss, L. A. *J. Comp. Chem.* **2001**, *22*, 976.
(31) Curtiss, L. A., Redfern, P. C., Rassolov, V. G., Kedziora, Pople, J. A. *J. Chem. Phys.* **2001**, *114*, 9287.
(32) Raghavachari, K.; Curtiss, L. A.; Rassolov, V.; Redfern, P. C., to be submitted.
(33) Frisch, M. J.; Trucks, G. W.; Schlegel, H. B.; Scuseria, G. E.; Robb, M. A.; Cheeseman, J. R.; Zakrzewski, V. G.; Montgomery Jr., J. A.; Stratmann, R. E.; Burant, J.; Dapprich, C. S.; Millam, J. M.; Daniels, A. D.; Kudin, K. N.; Strain, M. C.; Farkas, O.; Tomasi, J.; Barone, V.; Cossi, M.; Cammi, R.; Mennucci, B.; Pomelli, C.; Adamo, C.; Clifford, S.; Ochterski, J.; Petersson, G. A.; Ayala, P. Y.; Cui, Q.; Morokuma, K.; Malick, D. K.; Rabuck, A. D.; Raghavachari, K.; Foresman, J. B.; Cioslowski, J.; Ortiz, J. V.; Baboul, A. G.; Stefanov, B. B.; Liu, G.; Liashenko, A.; Piskorz, P.; Komaromi, I.; Gomperts, R.; Martin, R. L.; Fox, D. J.; Keith, T.; Al-Laham, M. A.; Peng, C. Y.; Nanayakkara, A.; Gonzalez, C.; Challacombe, M.; Gill, P. M. W.; Johnson, B.; Chen, W.; Wong, M. W.; Andres, J. L.; Gonzalez, C.; Head-Gordon, M.; Replogle, E. S.; Pople, J. A. *Gaussian 98*, Gaussian, Inc. Pittsburgh, PA, 1998.
(34) Saunders, V. R.; Dovesi, R.; Roetti, C.; Orlando, R.; Zicovich-Wilson, C. M.; Harrison, N. M.; Doll, K.; Civalleri, B.; Bush, I.; D'Arco, Ph.; Liunnell, M. CRYSTAL03 User's Manual, University of Torino, Torino, Italy, 2003.
(35) Bachmann, H. G.; Ahmed, F. R.; Barnes, W. H. *Z. Crystallogr.* **1961**, *115*, 110.
(36) Reed, A. E.; Curtiss, L. A.; Weinhold, F. *Chem. Rev.* **1988**, *88*, 899.
(37) Henkelman, G.; Jónsson, H. *J. Chem. Phys.* **2000**, *113*, 9978.
(38) Henkelman, G.; Uberuaga, B. P.; Jónsson, H. *J. Chem. Phys.* **2000**, *113*, 9901.
(39) Monkhorst, H. J.; Pack, J. D. *Phys. Rev.* **1976**, *13*, 5188.
(40) Tokarz-Sobieraj, R.; Witko, M.; Grybos, R. *Catal. Today* **2005**, *99*, 241.
(41) Engeser, M.; Schlangen, M.; Schröder, D.; Schwarz, H. *Organometallics* **2003**, *22*, 3933.
(42) Schröder, D.; Shaik, S.; Schwarz, H. *Acc. Chem. Res.* **2000**, *33*, 139.
(43) Dobler, J.; Pritsche, M.; Sauer, J. *J. Am. Chem. Soc.* **2005** *127*, 10861.
(44) Wachs, I. E.; Chen, Y.; Jehng, J.; Briand, L. E.; Tanaka, T. *Catal. Today* **2003**, *78*, 13.